Available online at www.sciencedirect.com
SCIENCE DIRECT®
Marine Structures 17 (2004) 435–454
MARINE STRUCTURES
www.elsevier.com/locate/marstruc

Hydroelastic analysis of a very large floating plate with large deflections in stochastic seaway ☆

Xu-jun Chen[a,b,c,*], J. Juncher Jensen[b], Wei-cheng Cui[c], Xue-feng Tang[a]

[a] *Engineering Institute of Engineering Crops, PLA University of Science and Technology, No. 1, Haifu Street, Nanjing 210007, China*
[b] *Department of Mechanical Engineering, Technical University of Denmark, DK-2800 Kgs. Lyngby, Denmark*
[c] *China Ship Scientific Research Center, Wuxi 214082, China*

Received 16 February 2004; received in revised form 7 September 2004; accepted 7 December 2004

Abstract

The hydroelasticity of a very large floating plate with large deflections in multidirectional irregular waves is discussed. After a brief introduction on wave loads on a flexible structure, the paper derives the generalised fluid force acting on a floating structure in multidirectional irregular waves. The nonlinear sectional forces induced by the membrane forces in the plate are deduced. The hydroelastic response equations of a floating plate with large deflections in multidirectional irregular waves are established, and a solution method in the frequency domain is discussed including extreme value statistics. A very large floating structure is chosen as an example. The numerical results show that the influence of the membrane forces on the vertical displacements and the bending moments is noticeable but not that large.

Keywords: Hydroelasticity; Floating plate; Membrane force; Irregular waves; Extreme value statistics

☆ The project was jointly supported by the National Natural Science Foundation of China (Grant No. 50039010, 50309018) and the Danish Rectors' Conference.

*Corresponding author. Engineering Institute of Engineering Crops, PLA University of Science and Technology, No. 1, Haifu Street, Nanjing 210007, China. Tel.:/fax: +86 25 84873355.
E-mail address: xjchen@sjtu.edu.cn (X.-j. Chen).

0951-8339/$ - see front matter
doi:10.1016/j.marstruc.2004.12.001

1. Introduction

Hydroelastic theories have been applied to the design and research works related to marine structures for several decades. Very large floating structures (VLFSs) require a hydroelastic analysis due to their large size [1–4]. Whereas both linear and nonlinear wave loads have been considered, nonlinear structural characteristics have generally not been included. However, as the maximum vertical displacement of a pontoon type very large floating structure may be larger than 1 m, the authors of this paper studied the hydroelasticity of a plate in multidirectional regular waves [5], where the membrane forces were taken into account. The numerical results showed that the membrane contribution both in terms of axial stresses and its effect on the bending stresses can be important. The paper was restricted to a bi-chromatic regular wave system considering only the sum-frequency contributions. In the present paper, the hydroelastic response equations of a floating plate with large deflections in multidirectional irregular waves are established and a solution method in the frequency domain is discussed. The nonlinear principal coordinates and their resonant characteristics are presented and extreme value statistics taking into account the kurtosis of the response are included.

2. Wave potential theory around a flexible floating structure

2.1. Decomposition of the velocity potential and the pressure

The fluid around a moored flexible floating body is assumed to be ideal (i.e., uniform, continuous, inviscid, incompressible and irrotational). Hence, the fluid behaviour can be modeled by a velocity potential. Two coordinate systems are introduced, namely a global equilibrium system $Oxyz$, and a body-fixed coordinate system $O'x'y'z'$. The origin of the $Oxyz$-system is at the point of intersection of the still water surface and the vertical line which goes through the gravity centre of the structure, and the Oz-axis is upward. The $O'x'y'z'$-system is fixed in the floating body.

The unsteady velocity potential $\phi(x,y,z,t)$ around a zero-forward speed floating structure in the equilibrium frame may be decomposed into the standard form (e.g., [6])

$$\phi(x,y,z,t) = \phi_I + \phi_D + \sum_{r=1}^{m} \phi_r, \tag{1}$$

where $\phi_I(x,y,z,t)$, $\phi_D(x,y,z,t)$ and $\phi_r(x,y,z,t)$ denote the incident wave potential, the diffraction wave potential, and the radiation wave potential arising from the responses of the flexible body. In the frequency domain, the first-order unsteady velocity potential and the principal coordinates $p_r(t)$ may be further expressed as

$$\phi(x,y,z,t) = \mathrm{Re}\left\{\left[\varphi_I(\omega) + \varphi_D(\omega) + \sum_{r=1}^{m} \varphi_r(\omega) p_r(\omega)\right] \mathrm{e}^{\mathrm{i}\omega t}\right\}, \tag{2}$$

$$p_r(t) = \mathrm{Re}\{p_r(\omega)\mathrm{e}^{\mathrm{i}\omega t}\}, \tag{3}$$

where ω is the wave circular frequency; $\varphi_I(x,y,z,\omega)$ and $\varphi_D(x,y,z,\omega)$ are the components of the incident wave velocity potential and the diffraction wave potential, respectively; $\varphi_r(x,y,z,\omega)$ $(r=1,\ldots,m)$ are the components of the radiation wave potential arising from the vibration in the rth principal dry mode of the flexible body, with unit amplitude and frequency ω. The potentials $\varphi_D(x,y,z,\omega)$ and $\varphi_r(x,y,z,\omega)$ are calculated using the Green function method [7]. p_r (ω) is the complex amplitude of the principal coordinate. The sign Re{ } in Eqs. (2) and (3) denotes the real part of the complex in { }.

The governing equations of the fluid are the Laplace equation and the Bernoulli equation. In the equilibrium coordinate system, they may be expressed as

$$\nabla^2\phi(x,y,z,t)=0, \tag{4}$$

$$\frac{p(x,y,z,t)}{\rho}+gz+\frac{\vec{v}\cdot\vec{v}}{2}+\frac{\partial\phi}{\partial t}=0. \tag{5}$$

$\vec{v}(x,y,z,t)$, $p(x,y,z,t)$ and ρ in Eq. (5) are respectively the velocity vector, the pressure and the density of the fluid. Finally, g is the acceleration of gravity.

The fluid pressure acting on the mean wetted surface S during the motion and distortion of the body is given by the Bernoulli equation in the equilibrium system

$$p(x,y,z,t)|_S=-\rho\left[\frac{\partial\phi}{\partial t}+\frac{\nabla\phi\cdot\nabla\phi}{2}+gz\right]_S. \tag{6}$$

The generalised forces acting on the floating structure associated with the model can be expressed as

$$Z_r(t)=-\iint_S \vec{n}\cdot\vec{u}_r^0 p\,\mathrm{d}S. \tag{7}$$

Here, $\vec{u}_r^0=(u_r^0,v_r^0,w_r^0)^T$, $(r=1,2,\ldots,m)$ is a set of orthogonal functions taken here as the dry modes of the plates and $\vec{n}$ is the normal vector of the wetted surface of the structure. In linear theory of hydroelasticity (e.g., [6,8]), $\vec{n}$ is taken to be independent of the motion. Thus, substitution of Eqs. (1) and (6) into Eq. (7) yields

$$Z_r(t)=Z_r^{(0)}+Z_r^{(1)}(t), \tag{8}$$

where $Z_r^{(0)}$ and $Z_r^{(1)}(t)$ are the generalised constant and first-order forces, respectively.

The constant forces are

$$Z_r^{(0)}=\rho\iint_S \vec{n}\cdot\vec{u}_r^0 gz\,\mathrm{d}S, \tag{9}$$

and provide the generalised steady state buoyancy forces.

The generalised first-order forces may be written as

$$Z_r^{(1)}(t)=E_r^{(1)}(t)+D_r^{(1)}(t)+R_r^{(1)}(t), \tag{10}$$

with

$$E_r^{(1)}(t)=\rho\iint_S \vec{n}\cdot\vec{u}_r^0\frac{\partial}{\partial t}[\phi_I(t)+\phi_D(t)]\,\mathrm{d}S, \tag{11}$$

$$D_r^{(1)}(t) = \sum_{k=1}^{m} \rho \iint_S \vec{n} \cdot \vec{u}_r^0 \frac{\partial}{\partial t} \phi_k(t) \, \mathrm{d}S, \tag{12}$$

$$R_r^{(1)}(t) = \rho \iint_S \vec{n} \cdot \vec{u}_r^0 \, gw \mathrm{d}S, \tag{13}$$

where $E_r^{(1)}(t)$, $H_r^{(1)}(t)$ and $R_r^{(1)}(t)$ are the generalised first-order wave exciting forces, radiation forces and restoring forces. w is the vertical displacement of the floating structure.

2.2. The generalised fluid forces in nonuniform waves

Assume that the nonuniform incident waves consist of multidirectional irregular waves, then

$$\phi_I(t) = \sum_{i=1}^{I} \sum_{j=1}^{J_i} \frac{g\zeta_{ji}}{\omega_{ji}} \mathrm{e}^{k_{ji}z} \sin[k_{ji}(x \cos \beta_i + y \sin \beta_i) - \omega_{ji}t + \varepsilon_{ji}], \tag{14}$$

where I is the number of direction of the nonuniform incident waves and β_i is the ith incident wave angle. The ith incident irregular waves are composed of J_i regular waves with the wave elevation ζ_{ji}, the wave circular frequency ω_{ji}, the wave number k_{ji} and the phase angle ε_{ji}.

Eq. (14) can also be expressed shortly as

$$\phi_I(t) = \sum_{j=1}^{N} \frac{g\zeta_j}{\omega_j} \mathrm{e}^{k_j z} \sin[k_j(x \cos \beta_j + y \sin \beta_j) - \omega_j t + \varepsilon_j], \tag{15}$$

where

$$N = \sum_{i=1}^{I} J_i \tag{16}$$

is the total number of regular waves in the flow field. $\zeta_j, \omega_j, k_j, \varepsilon_j$ and β_j are the wave elevation, the wave circular frequency, the wave number, the phase angle and the incident wave angle of the jth regular wave of the nonuniform waves.

By use of Eq. (15), the first-order wave potentials and the principal coordinates may be expressed as

$$\phi_I(x, y, z, t) = \mathrm{Re}\left[\sum_{j=1}^{N} \zeta_j \varphi_I(\omega_j) \mathrm{e}^{\mathrm{i}(\omega_j t + \varepsilon_j)}\right], \tag{17}$$

$$\phi_D(x, y, z, t) = \mathrm{Re}\left[\sum_{j=1}^{N} \zeta_j \varphi_D(\omega_j) \mathrm{e}^{\mathrm{i}(\omega_j t + \varepsilon_j)}\right], \tag{18}$$

$$p_k(t) = \mathrm{Re}\left[\sum_{j=1}^{N} \zeta_j p_k(\omega_j)\, \mathrm{e}^{\mathrm{i}(\omega_j t+\varepsilon_j)}\right], \tag{19}$$

$$\phi_k(x,y,z,t) = \mathrm{Re}\left[\sum_{j=1}^{N} \zeta_j p_k(\omega_j)\varphi_k(\omega_j)\, \mathrm{e}^{\mathrm{i}(\omega_j t+\varepsilon_j)}\right]. \tag{20}$$

Substituting Eqs. (17) and (18) into Eq. (11) gives the generalised first-order wave exciting forces

$$E_r^{(1)}(t) = \mathrm{Re}\left[\sum_{j=1}^{N} \zeta_j \xi_r(\omega_j)\, \mathrm{e}^{\mathrm{i}(\omega_j t+\varepsilon_j)}\right], \tag{21}$$

where $\xi_r(\omega_j)$, the coefficients of the generalised first-order wave exciting forces, can be expressed as

$$\xi_r(\omega_j) = \rho \iint_{\bar{S}} \vec{n} \cdot \vec{\bar{u}}_r^{0}(\mathrm{i}\omega_j)[\varphi_I(\omega_j) + \varphi_D(\omega_j)]\, \mathrm{d}S. \tag{22}$$

By substitution of Eq. (20) into Eq. (12) the first-order radiation forces are obtained:

$$D_r^{(1)}(t) = \mathrm{Re}\left\{\sum_{k=1}^{m}\sum_{j=1}^{N} \zeta_j[\omega_j^2 A_{rk}(\omega_j) - \mathrm{i}\omega_j B_{rk}(\omega_j)]p_k(\omega_j)\, \mathrm{e}^{\mathrm{i}(\omega_j t+\varepsilon_j)}\right\}, \tag{23}$$

where $A_{rk}(\omega_j)$ and $B_{rk}(\omega_j)$ are coefficients of added mass and added damping defined as

$$A_{rk}(\omega) = \frac{1}{\omega^2}\,\mathrm{Re}\left\{\mathrm{i}\rho \iint_{\bar{S}} \vec{n} \cdot \vec{\bar{u}}_r^{0}\omega\varphi_k(\omega)\, \mathrm{d}S\right\}. \tag{24}$$

$$B_{rk}(\omega) = \frac{i}{\omega}\,\mathrm{Im}$$

For a linear structure, the displacement of the structure can be expressed as

$$\vec{u}(t) = (u(t), v(t), w(t)) = \sum_{r=1}^{m} \vec{\bar{u}}_r^{0} p_r(t). \tag{25}$$

By substitution of Eqs. (19) and (25) into Eq. (13) the generalised first-order restoring forces are obtained

$$R_r^{(1)}(t) = \mathrm{Re}\left[\sum_{k=1}^{m} C_{rk} \sum_{j=1}^{N} \zeta_j p_k(\omega)\, \mathrm{e}^{\mathrm{i}(\omega_j t+\varepsilon_j)}\right], \tag{26}$$

where C_{rk} denotes the frequency independent coefficients of the generalised first-order forces expressed as

$$C_{rk} = \rho \iint_{\bar{S}} \vec{n} \cdot \vec{\bar{u}}_r^0 \, g w_k^0 \, \mathrm{d}S, \tag{27}$$

where w_k^0 is the kth vertical dry mode of the structure.

3. Equations of motion and solution methods

Based on the formulation of the generalised fluid forces acting on a three-dimensional flexible floating body, the equations of motion for solving the principal coordinates $p_s(t)$ may be represented as [9]

$$\sum_{s=1}^{m} [(a_{rs} + A_{rs})\ddot{p}_s(t) + (b_{rs} + B_{rs})\dot{p}_s(t) + (c_{rs} + C_{rs})p_s(t)] = E_r^{(1)}(t) + Z_r^{(0)} + Q_r, \quad r = 1, 2, \ldots, m, \tag{28}$$

where a_{rs}, b_{rs} and c_{rs} are the elements of the generalised mass matrix, the generalised damping matrix and the generalised stiffness matrix of the structure, respectively. These elements can together with the modes $\vec{\bar{u}}_r^0$ be obtained by a structural analysis program. Finally, Q_r denotes the generalised gravity forces.

According to the nonlinear von Karman plate equations (see e.g., [10]) and by omitting the gravity and static buoyancy forces, the hydroelastic equations for a uniform floating plate with large deflections can be written

$$\sum_{s=1}^{m_v} [(a_{rs} + A_{rs})\ddot{p}_s(t) + (b_{rs} + B_{rs})\dot{p}_s(t) + (c_{rs} + C_{rs})p_s(t)] = E_r^{(1)}(t) + H_r^{(s)}(t), \quad r = 1, 2, \ldots, m_v, \tag{29}$$

where m_v is the total number of vertical displacement modes of the floating plate. The extra term $H_r^{(s)}(t)$ on the right-hand side of Eq. (29) compared to Eq. (28) denotes the generalised nonlinear forces induced by the membrane forces in the plate [5] and will be discussed in the next section. Obviously, this term is a function of the principal coordinates $p_s(t)$.

By including only the leading nonlinear term, Eq. (29) can be solved in the frequency domain. The solution of Eq. (29) can be expressed as

$$p_s(t) = \sum_{j=1}^{N} [\zeta_j p_s^{(1)}(\omega_j) \, \mathrm{e}^{\mathrm{i}(\omega_j t + \varepsilon_j)}] + \frac{1}{4} \sum_{i=1}^{N} \sum_{j=1}^{N} \sum_{k=1}^{N} [\zeta_i \zeta_j \zeta_k p_s^{(s)}(\omega_{ijk}^{++}) \, \mathrm{e}^{\mathrm{i}(\omega_{ijk}^{++} t + \varepsilon_{ijk}^{++})}]$$

$$+\frac{1}{4}\sum_{i=1}^{N}\sum_{j=1}^{N}\sum_{k=1}^{N}[\zeta_i\zeta_j\zeta_k p_s^{(s)}(\omega_{ijk}^{+-})\,\mathrm{e}^{\mathrm{i}(\omega_{ijk}^{+-}t+\varepsilon_{ijk}^{+-})}]$$
$$+\frac{1}{4}\sum_{i=1}^{N}\sum_{j=1}^{N}\sum_{k=1}^{N}[\zeta_i\zeta_j\zeta_k p_s^{(s)}(\omega_{ijk}^{-+})\,\mathrm{e}^{\mathrm{i}(\omega_{ijk}^{-+}t+\varepsilon_{ijk}^{-+})}]$$
$$+\frac{1}{4}\sum_{i=1}^{N}\sum_{j=1}^{N}\sum_{k=1}^{N}[\zeta_i\zeta_j\zeta_k p_s^{(s)}(\omega_{ijk}^{--})\,\mathrm{e}^{\mathrm{i}(\omega_{ijk}^{--}t+\varepsilon_{ijk}^{--})}], \tag{30}$$

where

$$\begin{cases}\omega_{ijk}^{++}=\omega_i+\omega_j+\omega_k,\\ \omega_{ijk}^{+-}=\omega_i+\omega_j-\omega_k,\\ \omega_{ijk}^{-+}=\omega_i-\omega_j+\omega_k,\\ \omega_{ijk}^{--}=\omega_i-\omega_j-\omega_k,\end{cases}\quad\text{and}\quad\begin{cases}\varepsilon_{ijk}^{++}=\varepsilon_i+\varepsilon_j+\varepsilon_k,\\ \varepsilon_{ijk}^{+-}=\varepsilon_i+\varepsilon_j-\varepsilon_k,\\ \varepsilon_{ijk}^{-+}=\varepsilon_i-\varepsilon_j+\varepsilon_k,\\ \varepsilon_{ijk}^{--}=\varepsilon_i-\varepsilon_j-\varepsilon_k.\end{cases} \tag{31}$$

Furthermore, $p_s^{(1)}(\omega_j)$ denotes the first-order principal coordinates induced by the generalised first-order wave exciting forces. Only linear wave exciting forces are considered and thus second and high order exciting forces are neglected.

The second to fifth terms on the right-hand side of Eq. (30) are nonlinear contributions from the membrane forces. This will be discussed in the next section.

4. Generalised nonlinear force and contribution from the membrane forces

The nonlinear force vector induced by the large deflections dealt with in the von Karman plate theory is defined as (see e.g., [10])

$$H(t)=\frac{\partial^2F(t)}{\partial y^2}\frac{\partial^2w(t)}{\partial x^2}+\frac{\partial^2F(t)}{\partial x^2}\frac{\partial^2w(t)}{\partial y^2}-2\frac{\partial^2F(t)}{\partial x\partial y}\frac{\partial^2w(t)}{\partial x\partial y}, \tag{32}$$

where $w(t)$ is the vertical displacement of the plate, it can be the linear, the nonlinear or the combined one. $F(t)$ is the Airy stress function for the membrane stresses in the plate, satisfying

$$J_x\frac{\partial^4F(t)}{\partial x^4}+2J_{xy}\frac{\partial^4F(t)}{\partial x^2\partial y^2}+J_y\frac{\partial^4F(t)}{\partial y^4}=\left(\frac{\partial^2w(t)}{\partial x\partial y}\right)^2-\frac{\partial^2w(t)}{\partial x^2}\frac{\partial^2w(t)}{\partial y^2}, \tag{33}$$

with the boundary conditions

$$\frac{\partial^2F(t)}{\partial x\partial y}=0,\quad\frac{\partial^2F(t)}{\partial y^2}=0,\quad\text{at } x=\pm\frac{L}{2},$$
$$\frac{\partial^2F(t)}{\partial x\partial y}=0,\quad\frac{\partial^2F(t)}{\partial x^2}=0,\quad\text{at } y=\pm\frac{B}{2}. \tag{34}$$

Here, B and L are the width and the length of the floating plate. The constants J_x, J_{xy}, and J_y in Eq. (33) are the membrane flexibilities of the orthotropic plate. They are given as follows:

$$J_x = \frac{1}{E_y h^*}, \quad J_y = \frac{1}{E_x h^*}, \quad 2J_{xy} = \frac{1}{G_{xy} h^*} - v_x J_y - v_y J_x. \tag{35}$$

Here, h^* is the equivalent plate thickness, E_x and E_y are the equivalent Young's moduli of the material, G_{xy} is the equivalent shear modulus, and v_x, v_y are Poisson ratio coefficients.

The first-order complex displacements $w^{(1)}(t)$ can be calculated by

$$w^{(1)}(t) = \sum_{j=1}^{N} [\zeta_j w(\omega_j) \, \mathrm{e}^{\mathrm{i}[\omega_j t + \varepsilon_j]}], \tag{36}$$

where $w(\omega_j)$ is the complex amplitude of the displacement induced by the jth regular wave, determined by the first-order principal coordinate $p_s^{(1)}(\omega_j)$ and the dry modes w_s^0 of the plate

$$w(\omega_j) = \sum_{s=1}^{m_v} [w_s^0 p_s^{(1)}(\omega_j)]. \tag{37}$$

The dry modes w_s^0 can be calculated by any linear structural analysis code or, in the present case of a uniform plate, by analytical use of the orthotropic plate stiffnesses D_{11}, D_{12} and D_{22}.

Obviously, $w^{(1)}(t)$ shown in Eq. (36) is represented in complex form, and its conjugation can be expressed as

$$\overline{w^{(1)}(t)} = \sum_{j=1}^{N} [\zeta_j \overline{w(\omega_j)} \, \mathrm{e}^{-\mathrm{i}[\omega_j t + \varepsilon_j]}]. \tag{38}$$

Here and hereafter an over bar on a complex function or quantity represents its conjugation.

For simplification, the following relationship is introduced

$$\mathrm{Re}(X) \cdot \mathrm{Re}(Y) = \tfrac{1}{2}[\mathrm{Re}(X \cdot Y) + \mathrm{Re}(X \cdot \bar{Y})], \tag{39}$$

where X and Y are two arbitrary chosen complex functions or quantities.

By use of Eq. (39), substitution of Eqs. (36) and (38) into the right-hand side of Eq. (33) yields

$$\begin{aligned} & J_x \frac{\partial^4 F(t)}{\partial x^4} + 2J_{xy} \frac{\partial^4 F(t)}{\partial x^2 \partial y^2} + J_y \frac{\partial^4 F(t)}{\partial y^4} \\ & = \frac{1}{2} \mathrm{Re} \left\{ \sum_{i=1}^{N} \sum_{j=1}^{N} \zeta_i \zeta_j \left\langle \left[\frac{\partial^2 w(\omega_i)}{\partial x \partial y} \frac{\partial^2 w(\omega_j)}{\partial x \partial y} - \frac{\partial^2 w(\omega_i)}{\partial x^2} \frac{\partial^2 w(\omega_j)}{\partial y^2} \right] \mathrm{e}^{\mathrm{i}(\omega_{ij}^+ t + \varepsilon_{ij}^+)} \right. \right. \\ & \quad \left. \left. + \left[\frac{\partial^2 w(\omega_i)}{\partial x \partial y} \frac{\partial^2 \overline{w(\omega_j)}}{\partial x \partial y} - \frac{\partial^2 w(\omega_i)}{\partial x^2} \frac{\partial^2 \overline{w(\omega_j)}}{\partial y^2} \right] \mathrm{e}^{\mathrm{i}(\omega_{ij}^- t + \varepsilon_{ij}^-)} \right\rangle \right\}, \end{aligned} \tag{40}$$

where

$$\omega_{ij}^{\pm} = \omega_i \pm \omega_j, \quad \varepsilon_{ij}^{\pm} = \varepsilon_i \pm \varepsilon_j. \tag{41}$$

Eq. (40) can be solved by means of the boundary condition (34) by using the finite difference method [11]. The solution of Eq. (40) can be written as

$$F(t) = \frac{1}{2}\,\mathrm{Re}\left\{\sum_{i=1}^{N}\sum_{j=1}^{N}\zeta_i\zeta_j[F^{+}(\omega_i,\omega_j)\,\mathrm{e}^{\mathrm{i}(\omega_{ij}^{+}t+\varepsilon_{ij}^{+})} + F^{-}(\omega_i,\omega_j)\,\mathrm{e}^{\mathrm{i}(\omega_{ij}^{-}t+\varepsilon_{ij}^{-})}]\right\}. \tag{42}$$

By use of Eq. (39), substitution of the Eqs. (36), (38) and (42) into (32) yields

$$\begin{aligned} H(t) = \frac{1}{4}\,\mathrm{Re}\Bigg\{\sum_{i=1}^{N}\sum_{j=1}^{N}\sum_{k=1}^{N}\zeta_i\zeta_j\zeta_k[&H^{++}(\omega_i,\omega_j,\omega_k)\,\mathrm{e}^{\mathrm{i}(\omega_{ijk}^{++}t+\varepsilon_{ijk}^{++})} \\ &+ H^{+-}(\omega_i,\omega_j,\omega_k)\,\mathrm{e}^{\mathrm{i}(\omega_{ijk}^{+-}t+\varepsilon_{ijk}^{+-})} + H^{-+}(\omega_i,\omega_j,\omega_k)\,\mathrm{e}^{\mathrm{i}(\omega_{ijk}^{-+}t+\varepsilon_{ijk}^{-+})} \\ &+ H^{--}(\omega_i,\omega_j,\omega_k)\,\mathrm{e}^{\mathrm{i}(\omega_{ijk}^{--}t+\varepsilon_{ijk}^{--})}]\Bigg\}, \end{aligned} \tag{43}$$

where

$$\begin{aligned} H^{++}(\omega_i,\omega_j,\omega_k) = {} & \frac{\partial^2 F^{+}(\omega_i,\omega_j)}{\partial y^2}\frac{\partial^2 w(\omega_k)}{\partial x^2} + \frac{\partial^2 F^{+}(\omega_i,\omega_j)}{\partial x^2}\frac{\partial^2 w(\omega_k)}{\partial y^2} \\ & - 2\frac{\partial^2 F^{+}(\omega_i,\omega_j)}{\partial x\partial y}\frac{\partial^2 w(\omega_k)}{\partial x\partial y}, \end{aligned}$$

$$\begin{aligned} H^{+-}(\omega_i,\omega_j,\omega_k) = {} & \frac{\partial^2 F^{+}(\omega_i,\omega_j)}{\partial y^2}\frac{\partial^2 \overline{w(\omega_k)}}{\partial x^2} + \frac{\partial^2 F^{+}(\omega_i,\omega_j)}{\partial x^2}\frac{\partial^2 \overline{w(\omega_k)}}{\partial y^2} \\ & - 2\frac{\partial^2 F^{+}(\omega_i,\omega_j)}{\partial x\partial y}\frac{\partial^2 \overline{w(\omega_k)}}{\partial x\partial y}, \end{aligned}$$

$$\begin{aligned} H^{-+}(\omega_i,\omega_j,\omega_k) = {} & \frac{\partial^2 F^{-}(\omega_i,\omega_j)}{\partial y^2}\frac{\partial^2 w(\omega_k)}{\partial x^2} + \frac{\partial^2 F^{-}(\omega_i,\omega_j)}{\partial x^2}\frac{\partial^2 w(\omega_k)}{\partial y^2} \\ & - 2\frac{\partial^2 F^{-}(\omega_i,\omega_j)}{\partial x\partial y}\frac{\partial^2 w(\omega_k)}{\partial x\partial y}, \end{aligned}$$

$$\begin{aligned} H^{--}(\omega_i,\omega_j,\omega_k) = {} & \frac{\partial^2 F^{-}(\omega_i,\omega_j)}{\partial y^2}\frac{\partial^2 \overline{w(\omega_k)}}{\partial x^2} + \frac{\partial^2 F^{-}(\omega_i,\omega_j)}{\partial x^2}\frac{\partial^2 \overline{w(\omega_k)}}{\partial y^2} \\ & - 2\frac{\partial^2 F^{-}(\omega_i,\omega_j)}{\partial x\partial y}\frac{\partial^2 \overline{w(\omega_k)}}{\partial x\partial y}. \end{aligned} \tag{44}$$

The generalised nonlinear forces can hence be expressed as

$$H_r(t) = \frac{1}{4}\,\mathrm{Re}\Bigg\{\sum_{i=1}^{N}\sum_{j=1}^{N}\sum_{k=1}^{N}\zeta_i\zeta_j\zeta_k[H_r^{++}(\omega_i,\omega_j,\omega_k)\,\mathrm{e}^{\mathrm{i}(\omega_{ijk}^{++}t+\varepsilon_{ijk}^{++})} + H_r^{+-}(\omega_i,\omega_j,\omega_k)\,\mathrm{e}^{\mathrm{i}(\omega_{ijk}^{+-}t+\varepsilon_{ijk}^{+-})} + H_r^{-+}(\omega_i,\omega_j,\omega_k)\,\mathrm{e}^{\mathrm{i}(\omega_{ijk}^{-+}t+\varepsilon_{ijk}^{-+})} + H_r^{--}(\omega_i,\omega_j,\omega_k)\,\mathrm{e}^{\mathrm{i}(\omega_{ijk}^{--}t+\varepsilon_{ijk}^{--})}]\Bigg\}, \tag{45}$$

where

$$H_r^*(\omega_i,\omega_j,\omega_k) = \sum_{n=1}^{N_p} w_r^{(n)} H^{*(n)}(\omega_i,\omega_j,\omega_k), \tag{46}$$

and where $w_r^{(n)}$ and $H^{*(n)}$ are the rth vertical mode and the nonlinear forces acting on node n. N_p is the total number of nodes included for the plate. H_r^* and $H^{*(n)}$ denotes H_r^{++}, H_r^{+-}, H_r^{-+} or H_r^{--} and $H^{++(n)}$, $H^{+-(n)}$, $H^{-+(n)}$ or $H^{--(n)}$, respectively.

With the generalised nonlinear forces induced by the membrane forces given by Eq. (32), the following equation is solved to obtain the third-order principal coordinates $p_s^{(s)}(\omega_{ijk}^*)$:

$$\sum_{s=1}^{m_v}[-(\omega_{ijk}^*)^2(a_{rs}+A_{rs}) + (i\omega_{ijk}^*)(b_{rs}+B_{rs}) + (c_{rs}+C_{rs})]p_s^{(s)}(\omega_{ijk}^*) = H_r^*(\omega_i,\omega_j,\omega_k), \quad (r=1,2,\ldots,m_v)\ (i,j,k=1,\ldots,N). \tag{47}$$

Here and hereafter superscript ω_{ijk}^* denotes ω_{ijk}^{++}, ω_{ijk}^{+-}, ω_{ijk}^{-+} or ω_{ijk}^{--}. The first-order hydrodynamic coefficients A_{rs} and B_{rs} are calculated by use of Eq. (24) at the corresponding frequencies $|\omega_{ijk}^*|$. Thus $p_s^{(s)}(\omega_{ijk}^*)$ are nonlinear functions of the linear principal coordinates $p_s^{(1)}(\omega_j)$. It should be noted that when $\omega_{ijk}^* = 0$, Eq. (47) becomes

$$\sum_{s=1}^{m_v}(c_{rs}+C_{rs})p_s^{(s)}(\omega_{ijk}^*) = H_r^*(\omega_i,\omega_j,\omega_k), \quad (r=1,2,\ldots,m_v)\ (i,j,k=1,\ldots,N). \tag{48}$$

With the expression of the total principal coordinates shown in Eq. (30), the total displacements can be calculated by

$$w(t) = \mathrm{Re}\Bigg\{\sum_{s=1}^{m_v}[w_s^0 p_s(t)]\Bigg\} = \mathrm{Re}\Bigg[\sum_{j=1}^{N}\Bigg\{\zeta_j\,\mathrm{e}^{\mathrm{i}(\omega_j t+\varepsilon_j)}\sum_{s=1}^{m_v}[w_s^0 p_s^{(1)}(\omega_j)]\Bigg\} + \frac{1}{4}\sum_{i=1}^{N}\sum_{j=1}^{N}\sum_{k=1}^{N}\Bigg\{\zeta_i\zeta_j\zeta_k\,\mathrm{e}^{\mathrm{i}(\omega_{ijk}^{++}t+\varepsilon_{ijk}^{++})}\sum_{s=1}^{m_v}[w_s^0 p_s^{(s)}(\omega_{ijk}^{++})]\Bigg\} + \frac{1}{4}\sum_{i=1}^{N}\sum_{j=1}^{N}\sum_{k=1}^{N}\Bigg\{\zeta_i\zeta_j\zeta_k\,\mathrm{e}^{\mathrm{i}(\omega_{ijk}^{+-}t+\varepsilon_{ijk}^{+-})}\sum_{s=1}^{m_v}[w_s^0 p_s^{(s)}(\omega_{ijk}^{+-})]\Bigg\}$$

$$+\frac{1}{4}\sum_{i=1}^{N}\sum_{j=1}^{N}\sum_{k=1}^{N}\left\{\zeta_i\zeta_j\zeta_k\,\mathrm{e}^{\mathrm{i}(\omega_{ijk}^{-+}t+\varepsilon_{ijk}^{-+})}\sum_{s=1}^{m_v}[w_s^0 p_s^{(s)}(\omega_{ijk}^{-+})]\right\}$$
$$+\frac{1}{4}\sum_{i=1}^{N}\sum_{j=1}^{N}\sum_{k=1}^{N}\left\{\zeta_i\zeta_j\zeta_k\,\mathrm{e}^{\mathrm{i}(\omega_{ijk}^{--}t+\varepsilon_{ijk}^{--})}\sum_{s=1}^{m_v}[w_s^0 p_s^{(s)}(\omega_{ijk}^{--})]\right\}\Bigg]. \tag{49}$$

With the displacements, all the other parameters related to the fluid and the structure can be calculated. For example, the bending moments in the plate become

$$M_x=-D_{11}\left[\frac{\partial^2 w(t)}{\partial x^2}+v_y\frac{\partial^2 w(t)}{\partial y^2}\right],$$

$$M_y=-D_{22}\left[\frac{\partial^2 w(t)}{\partial y^2}+v_x\frac{\partial^2 w(t)}{\partial x^2}\right],$$

$$M_{xy}=-2D_{12}\left[\frac{\partial^2 w(t)}{\partial x\partial y}\right]. \tag{50}$$

Here, D_{11}, D_{12} and D_{22} are the orthotropic plate stiffnesses.

5. Numerical solution

5.1. Particulars of the incident waves and the floating plate

For simplicity, two identical irregular wave systems are coming from different directions and assumed to act on a very large floating plate. The wave energy spectrum of each system is shown in Fig. 1. Each of the irregular waves is approximated by 17 regular waves as indicated in Fig. 1. The peak frequency of the irregular wave is 1.12 rad/s. The significant wave height of each irregular wave is 2 m.

The particulars of the VLFS mentioned by Sim and Choi [12] are chosen as an example. The relevant data is shown in Table 1. The VLFS is a scaled model of the Mega-Float constructed and developed in Yokosuka [13] and to be used close to land in sheltered waters. In Sim and Choi [12] the bending rigidity is given to be $EI=4.77\times10^{11}\,\mathrm{Nm}^2$. If an isotropic plate of the thickness $h=2.0\,\mathrm{m}$ is assumed, this bending rigidity corresponds to an equivalent Young's modulus $E=1.19\times10^{10}\,\mathrm{N/m}^2$. As no information on the structural layout of this VLFS is given in the open literature, the structure is assumed to be made of steel and composed of a set of crossing webs spaced both longitudinally and transversely by 3 m. The equivalent thickness of the webs is taken to be 12.9 mm whereas the equivalent thickness of the bottom and top plates is taken to be 17.5 mm. The mass of local stiffening and nonstructural items is accounted for by increasing the mass of the steel structure by 25 per cent and hence the draught of the VLFS becomes 0.5 m. The resulting membrane stiffness Eh^* corresponds to an equivalent plate thickness of approximately 0.766 m. It should be stressed that shear deformations are neglected even if

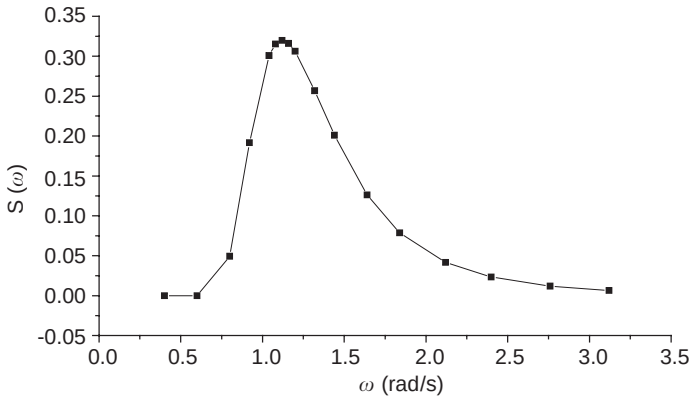

Fig. 1. Wave energy spectrum of the irregular waves.

Table 1
Particulars of the plate

Length L	300.0 m
Width B	60.0 m
Depth h	2.0 m
Equivalent plate thickness h^*	0.766 m
Draught d	0.5 m
Young's modulus E	1.19×10^{10} N/m^2
Poisson's ratio v	0.13
Mass density ρ_b	256.25 kg/m^3

they might be just as important as the membrane effects for the present structure. A total number of modes $m = 22$ (3 rigid ones and 19 elastic ones) is applied.

5.2. Analysis of the nonlinear coordinates

Figs. 2–5 show selected nonlinear principal coordinates $p_s^{(s)}(\omega_{ijk}^*)$ of the first four vertical bending moment modes. Resonant vibrations are seen in them, e.g. Fig. 2 (first-order), Fig. 3 (second-order), Fig. 4 (third-order) and Fig. 5 (fourth-order). The differences in vertical scales should be noted. The figures show for example that the maximum principal of the fourth-order resonant vibrations (0.0000014) is far smaller than that of the first-order resonant vibrations (0.012). A total number of 22 modes is found suitable for the numerical example. The wave angles are $\beta_1 = 45^\circ$ and $\beta_2 = -45^\circ$, respectively. The horizontal axes are integer numbers where each number denotes a certain combination of ω_i, ω_j and ω_k satisfying $\omega_i \pm \omega_j \pm \omega_k = \text{constant}$. This is the reason for the repetitive pattern visible in the figures as it just corresponds

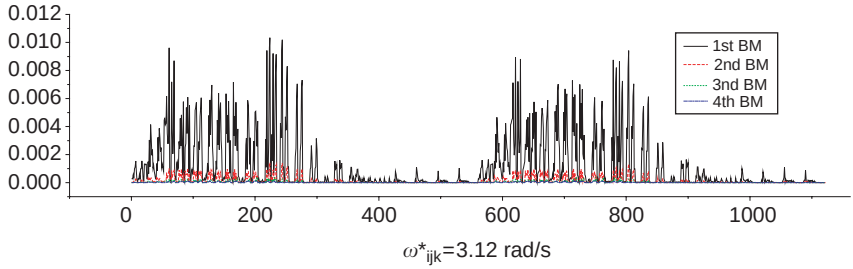

Fig. 2. First-order resonant vibration of vertical bending moment $\omega^*_{ijk} = 3.12\,\mathrm{rad/s}$.

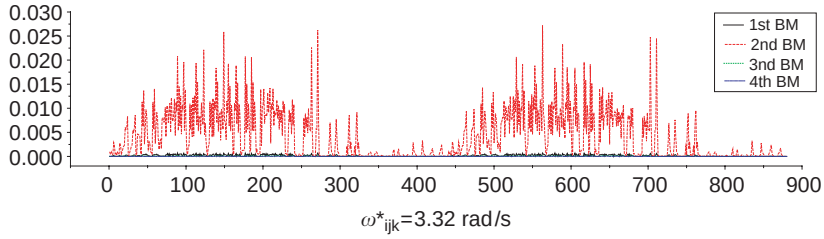

Fig. 3. Second-order resonant vibration of vertical bending moment $\omega^*_{ijk} = 3.32\,\mathrm{rad/s}$.

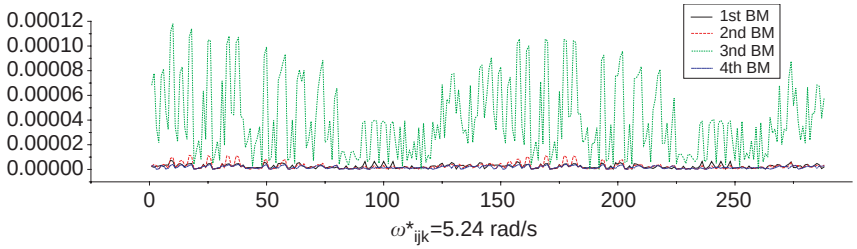

Fig. 4. Third-order resonant vibration of vertical bending moment $\omega^*_{ijk} = 5.24\,\mathrm{rad/s}$.

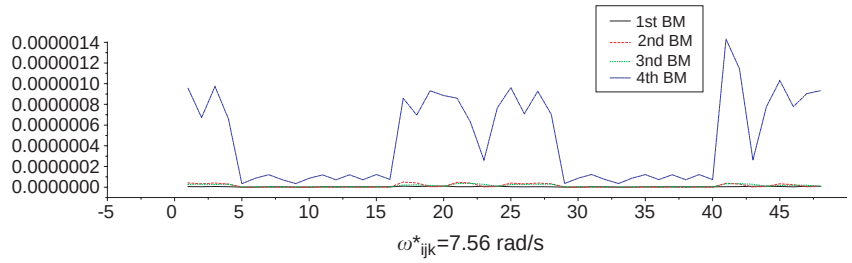

Fig. 5. Fourth-order resonant vibration of vertical bending moment $\omega^*_{ijk} = 7.56\,\mathrm{rad/s}$.

Table 2
Resonant vibration frequencies

r	$A_{rr}(\omega_{ijk}^{+})/10^6$	$a_{rr}/10^6$	$c_{rr}/10^6$	$C_{rr}/10^6$	$\omega_{s_{r-6}}$/rad/s	ω_{w_r}/rad/s
7	2.575	2.302	2.211	45.050	0.980	3.113
8	3.274	2.290	16.753	44.578	2.705	3.320
10	1.643	2.266	63.867	43.793	5.309	5.248
12	1.577	2.232	172.239	42.676	8.785	7.512

to interchange of the indices i, j and k. The lines drawn between the points are only used to make the figures more readable.

The elastic resonant vibration frequencies ω_{w_r} in water are calculated by Eq. (51) below [9] and the results of the first four vertical bending moment modes are shown in Table 2, where $\omega_{s_{r-6}}$ denotes the natural frequencies of the elastic responses in air. $A_{rr}(\omega_{ijk}^{+})$ are diagonal elements of the non-diagonal generalised added mass matrix (in SI units).

$$-\omega_{w_r}^2[a_{rr} + A_{rr}(\omega_{ijk}^{+})] + (c_{rr} + C_{rr}) = 0. \tag{51}$$

5.3. Extreme value predictions of bending moments

As the phase angle components ε_j and ε_{ijk}^{*} in Eq. (30) are random variables, the principal coordinates, the vertical displacements and the bending moments are all random variables. Because a stationary sea state is considered, extreme value predication can be performed on the basis of the theory of stationary stochastic processes.

For a stationary stochastic process, we may set $t = 0$ in Eq. (49) which yields

$$w = \sum_{j=1}^{2N} \lambda_j \xi_j + \sum_{i=1}^{2N}\sum_{j=1}^{2N}\sum_{k=1}^{2N} \Lambda_{ijk}\xi_i\xi_j\xi_k, \tag{52}$$

where

$$\lambda_j = \begin{cases} \mathrm{Re}\left\{\sum_{s=1}^{m_v} w_s^0 p_s^{(1)}(\omega_j)\right\} \\ \\ -\mathrm{Im}\left\{\sum_{s=1}^{m_v} w_s^0 p_s^{(1)}(\omega_{j-N})\right\} \end{cases}, \quad \xi_j = \begin{cases} \zeta_j \cos\varepsilon_j \\ \zeta_j \sin\varepsilon_j \end{cases} \text{ when } \begin{cases} j \leqslant N \\ j > N \end{cases}, \tag{53}$$

$$\Lambda_{ijk} = \begin{cases} \dfrac{1}{4}\,\mathrm{Re}\left\{\sum_{s=1}^{m_v} w_s^0[p_s^{(s)}(\omega_{i'j'k'}^{++}) + p_s^{(s)}(\omega_{i'j'k'}^{+-}) + p_s^{(s)}(\omega_{i'j'k'}^{-+}) + p_s^{(s)}(\omega_{i'j'k'}^{--})]\right\}, \\ \quad \text{when } i,j,k \leqslant N, \\ -\dfrac{1}{4}\,\mathrm{Re}\left\{\sum_{s=1}^{m_v} w_s^0[p_s^{(s)}(\omega_{i'j'k'}^{++}) + p_s^{(s)}(\omega_{i'j'k'}^{+-}) + p_s^{(s)}(\omega_{i'j'k'}^{-+}) + p_s^{(s)}(\omega_{i'j'k'}^{--})]\right\}, \\ \quad \text{only one of } i,j,k \leqslant N, \\ -\dfrac{1}{4}\,\mathrm{Im}\left\{\sum_{s=1}^{m_v} w_s^0[p_s^{(s)}(\omega_{i'j'k'}^{++}) + p_s^{(s)}(\omega_{i'j'k'}^{+-}) + p_s^{(s)}(\omega_{i'j'k'}^{-+}) + p_s^{(s)}(\omega_{i'j'k'}^{--})]\right\}, \\ \quad \text{only one of } i,j,k > N, \\ \dfrac{1}{4}\,\mathrm{Im}\left\{\sum_{s=1}^{m_v} w_s^0[p_s^{(s)}(\omega_{i'j'k'}^{++}) + p_s^{(s)}(\omega_{i'j'k'}^{+-}) + p_s^{(s)}(\omega_{i'j'k'}^{-+}) + p_s^{(s)}(\omega_{i'j'k'}^{--})]\right\}, \\ \quad \text{when } i,j,k > N, \end{cases} \tag{54}$$

where

$$i' = \begin{cases} i \\ i-N \end{cases}, \quad \begin{cases} i \leqslant N \\ i > N \end{cases}, \quad j' = \begin{cases} j \\ j-N \end{cases}, \quad \begin{cases} j \leqslant N \\ j > N \end{cases},$$
$$k' = \begin{cases} k \\ k-N \end{cases}, \quad \begin{cases} k \leqslant N \\ k > N \end{cases}. \tag{55}$$

Substitution of Eq. (52) into (50) yields

$$M_x = \sum_{j=1}^{2N} \alpha_j \xi_j + \sum_{i=1}^{2N}\sum_{j=1}^{2N}\sum_{k=1}^{2N} \beta_{ijk}\xi_i\xi_j\xi_k, \tag{56}$$

where

$$\alpha_j = -D_{11}\left(\frac{\partial^2 \lambda_j}{\partial x^2} + v_y \frac{\partial^2 \lambda_j}{\partial y^2}\right), \tag{57}$$

$$\beta_{ijk} = -D_{11}\left(\frac{\partial^2 \Lambda_{ijk}}{\partial x^2} + v_y \frac{\partial^2 \Lambda_{ijk}}{\partial y^2}\right). \tag{58}$$

The bending moments M_y and M_{xy} have expressions similar to Eq. (56).

The central moments $\eta_1 = E[M_x]$ and $\eta_n = E\lfloor (M_x - \eta_1)^n \rfloor$ of the bending moment distribution can be expressed as [14]:

$$\eta_1 = 0,$$

$$\eta_2 = \sum_{i=1}^{2N} \alpha_i \alpha_i V_i + \sum_{i=1}^{2N} \sum_{j=1}^{2N} \sum_{k=1}^{2N} (9\beta_{ijj}\beta_{ikk} + 6\beta_{ijk}\beta_{ijk}) V_i V_j V_k + 6 \sum_{i=1}^{2N} \sum_{j=1}^{2N} \alpha_i \beta_{ijj} V_i V_j,$$

$$\eta_3 = 0,$$

$$\eta_4 = 3\eta_2^2 + 24 \sum_{i=1}^{2N} \sum_{j=1}^{2N} \sum_{k=1}^{2N} \alpha_i \alpha_j \alpha_k \beta_{ijk} V_i V_j V_k, \tag{59}$$

where

$$V_i = E[\xi_i \xi_i] = S(\omega_i)\Delta\omega_i \tag{60}$$

is the variance of ξ_i [15]. The statistics of the bending moments can be calculated by use of a Gram–Charlier expansion [14]. However, a simple cubic approximation $\widetilde{M}_x$ for M_x

$$\widetilde{M}_x = c_1 U + c_3 U^3, \tag{61}$$

where c_1 and c_3 are determined so that

$$\mathrm{E}[\widetilde{M}_x^2] = \mathrm{E}[M_x^2] = \eta_2,$$

$$\mathrm{E}[\widetilde{M}_x^4] = \mathrm{E}[M_x^4] = \eta_4, \tag{62}$$

taking U to be a standard normal distribution variable is usually preferred. The reason is that the Gram–Charlier series often yields negative probability densities in the tail of the distribution. As the wave process is rather narrow-banded the peak values of U can be assumed to follow a Rayleigh distribution, and thus the most probable largest peak of U among N_z peaks becomes $\sqrt{2\ln N_z}$.

For the nonlinear distribution of M_x considered in the present paper, the most probable largest bending moment during a finite time $t = N_z T_z$ then becomes

$$M_x^e = c_1\sqrt{2\ln N_z} + c_3(\sqrt{2\ln N_z})^3, \tag{63}$$

where T_z is the zero-upcrossing period. The coefficients c_1 and c_3 in Eq. (63) can be determined from the following nonlinear equations [16]:

$$\eta_2 = c_1^2 + 6c_1c_3 + 15c_3^2,$$

$$\eta_4 = 3c_1^4 + 10395c_3^4 + 630c_1^2c_3^2 + 3780c_1c_3^3 + 60c_1^3c_3. \tag{64}$$

Based on the theory shown in Eqs. (51)–(64), the predicted most probable extreme values of bending moments at 11 selected points for an operational period of 1–20 years (the grid of the plate and the coordinates of the points are shown in Fig. 6 and Table 3) are calculated and some results are given in Figs. 7–12. The wave angles are $\beta_1 = 45^\circ$, $\beta_2 = -45^\circ$ and $\beta_1 = 45^\circ$, $\beta_2 = 135^\circ$, respectively.

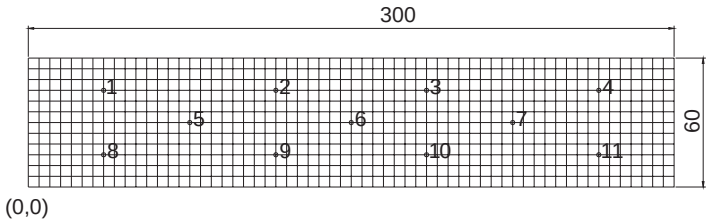

Fig. 6. Grid of the plate.

Table 3
Coordinates of the selected points

1	2	3	4	5	6	7	8	9	10	11
(35,45)	(115,45)	(185,45)	(265,45)	(75,30)	(150,30)	(225,30)	(35,15)	(115,15)	(185,15)	(265,15)

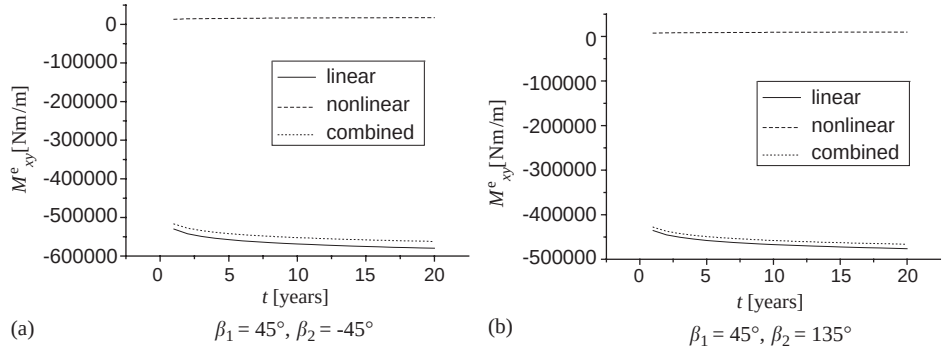

Fig. 7. Predicted extreme value of bending moment M^e_{xy} of point 1: (a) $\beta_1 = 45°$, $\beta_2 = -45°$, (b) $\beta_1 = 45°$, $\beta_2 = 135°$.

From the figures and the numerical results it is seen that

(a) The membrane forces have a small, but different influence on the bending moments of different points.
(b) Wave angles have an influence on the predicted extreme values. For $\beta_1 = 45°$, $\beta_2 = 135°$, the maximum nonlinear effects on the extreme bending moments M^e_x, M^e_y and M^e_{xy} for a period of 20 years are -0.02%, -1.9% and -2.4%, respectively. For $\beta_1 = 45°$, $\beta_2 = -45°$, the maximum effects on the extreme bending moments M^e_x, M^e_y and M^e_{xy} for a period of 20 years are 0.02%, -2.0% and -3.09%, respectively.

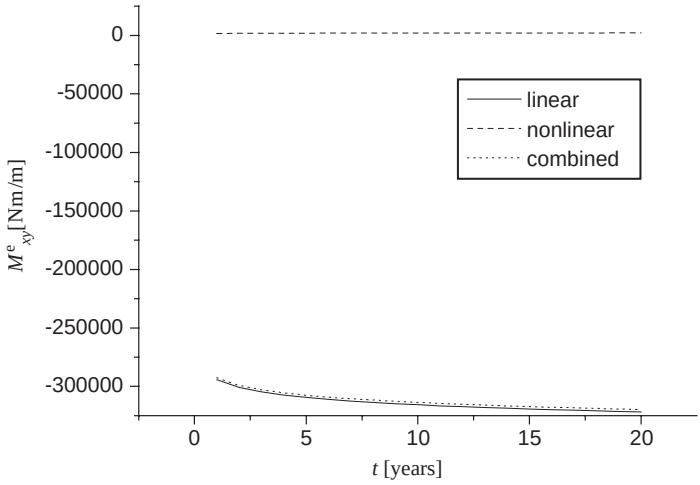

Fig. 8. Predicted extreme value of bending moment M^e_{xy} of point 4 ($\beta_1 = 45^\circ,\ \beta_2 = -45^\circ$).

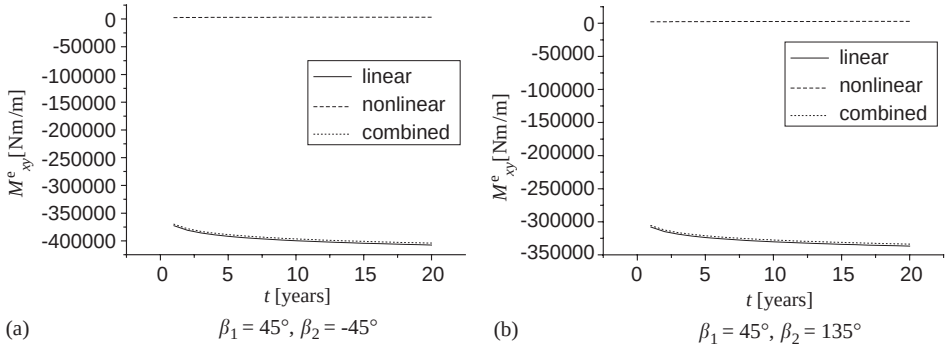

Fig. 9. Predicted extreme value of bending moment M^e_{xy} of point 5: (a) $\beta_1 = 45^\circ,\ \beta_2 = -45^\circ$, (b) $\beta_1 = 45^\circ,\ \beta_2 = 135^\circ$.

6. Conclusions

The objective of the paper has been to investigate the membrane effect in VLFS of the pontoon type subjected to stochastic wave loads. In the analysis linear incident waves are assumed and the nonlinearities in the response are solely due to the coupling between axial forces and bending moments. This coupling is modeled by the von Karman plate equations.

The numerical solution is found in the frequency domain taking only the lowest order of nonlinearity into account. The nonlinear responses involve sum and differences combinations of three wave components. These components are determined numerically using the concept of principal modes which allows a quick identification of the resonance modes. The nonlinear response is symmetric with a

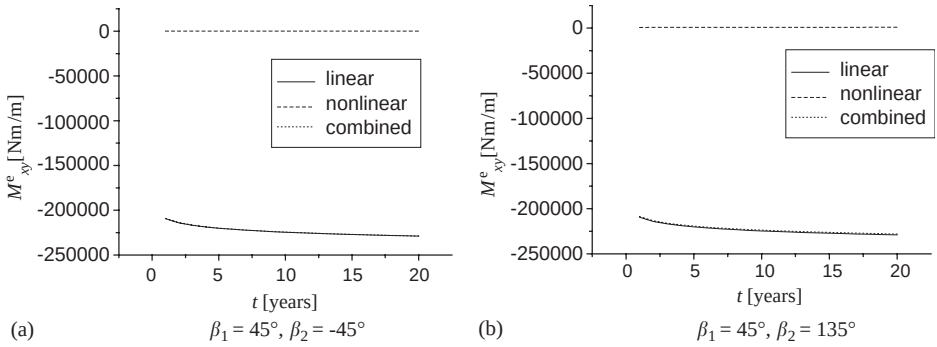

Fig. 10. Predicted extreme value of bending moment M^e_{xy} of point 6: (a) $\beta_1 = 45^\circ,\ \beta_2 = -45^\circ$, (b) $\beta_1 = 45^\circ,\ \beta_2 = 135^\circ$.

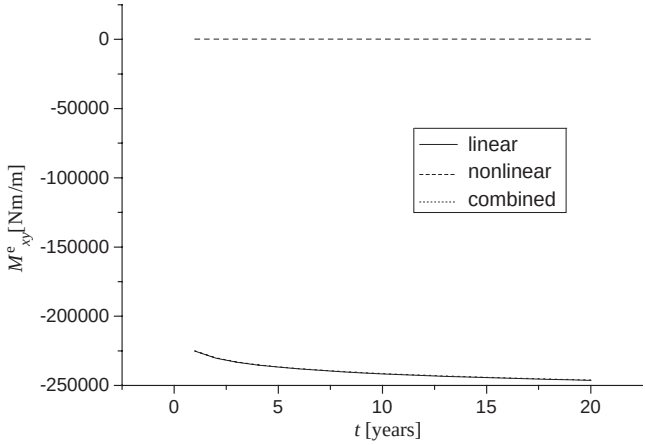

Fig. 11. Predicted extreme value of bending moment M^e_{xy} of point 7 ($\beta_1 = 45^\circ,\ \beta_2 = -45^\circ$).

kurtosis different from a Gaussian distribution. Extreme values of the response are determined by a Hermite transformation involving the variance and the kurtosis of the response.

From the numerical example it is found that for a typical VLFS pontoon configuration the membrane effects are very modest, decreasing the extreme bending moment by a few percent. The conclusion is slightly different from Chen et al., considering regular waves [5].

The wave loads are treated by a linear procedure and further studies should be performed to assess the importance of nonlinear wave load components. Also shear deformations ought to be considered in future work.

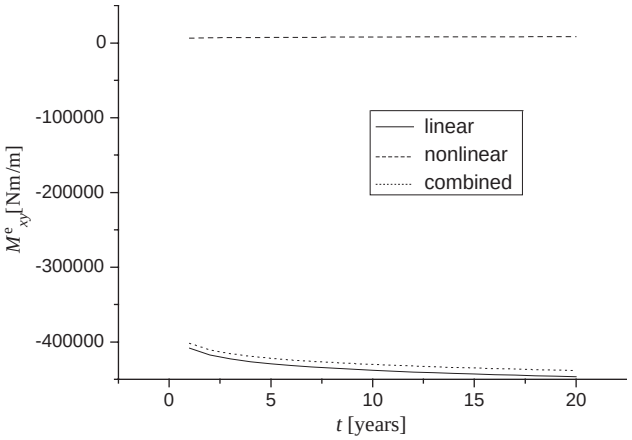

Fig. 12. Predicted extreme value of bending moment M^e_{xy} of point 8 ($\beta_1 = 45^\circ$, $\beta_2 = 135^\circ$).

References

[1] Ertekin RC, Riggs HR. Proceedings of the first international workshop on very large floating structures-VLFS'91, Honolulu, Hawaii, USA, 1991.
[2] Ertekin RC, Riggs HR. Proceedings of the third international workshop on very large floating structures-VLFS'99, Honolulu, Hawaii, USA, 1999.
[3] Watanabe Y. Proceedings of the second international workshop on very large floating structures-VLFS'96, Hayama, Japan, November 25–28, 1996.
[4] Kashiwagi M, Koterayama W, Ohkusu M. Hydroelasticity in marine technology. Proceedings of the second international conference on hydroelasticity in marine technology, Fukuoka, Japan, 1998.
[5] Chen XJ, Jensen JJ, Cui WC, Fu SX. Hydroelasticity of a floating plate in multi-directional waves. Ocean Eng 2003;30(15):1997–2017.
[6] Wu YS. Hydroelasticity of floating bodies. PhD thesis, Brunel University, UK, 1984.
[7] Newman JN. Marine hydrodynamics. Cambridge, MA: MIT Press; 1986.
[8] Price WG, Wu YS. Structural responses of a SWATH of multi-hulled vessel travelling in waves. International conference on SWATH ships and advanced multi-hulled vessels, RINA, London, 1985.
[9] Chen XJ, Wu YS, Cui WC, Tang XF. Nonlinear hydroelastic analysis of a moored floating body. Ocean Eng 2003;30(8):965–1003.
[10] Brush DO, Almroth BO. Buckling of bars, plates and shells. USA: Kingsport Press; 1975.
[11] Chen XJ, Cui WC, Song H, Tang XF. Numerical solution of membrane forces for a free–free floating plate with large deflection. China Ocean Engineering 2003;17(2):163–76.
[12] Sim IH, Choi HS. An analysis of the hydroelastic behavior of large floating structures in oblique waves. Hydroelasticity in marine technology. Proceedings of the second international conference on hydroelasticity in marine technology, Fukuoka, Japan, 1998. p. 195–9.
[13] Yago K, Endo H. Model experiment and numerical calculation of the hydroelastic behavior of matlike VLFS. Proceedings of the second international workshop on very large floating structures-VLFS'96, Hayama, Japan, 1996.
[14] Longuet-Higgins MS. The effect of non-linearities on statistical distributions in the theory of sea waves. J Fluid Mech 1964;17:459–80.
[15] Jensen JJ, Dogliani M. Wave-induced ship hull vibrations on stochastic seaways. Marine Struct 1996;9(3–4):353–87.
[16] Jensen JJ. Load and global response of ships. Elsevier ocean engineering book series, vol. 4. UK: Elsevier Science, 2001.